Theoretical studies of the interaction between silver and lipids present in HepG2 cells

Pamela C. Ubaldo and Lichang Wang*

Department of Chemistry and Biochemistry, Southern Illinois University Carbondale, Carbondale, IL 62901, USA

Abstract

We performed DFT and TDDFT calculations to determine interactions between silver atom and model cell membrane of human hepatocellular carcinoma (HepG2) cells or human liver cells. Specifically, we chose the two major lipid constituents of HepG2 cells which are 1-palmitoyl-2-oleoyl-sn-glycero-3-phosphocholine (POPC) and 1-palmitoyl-2-oleoyI-sn-glycero-3-phosphoethanolamine (POPE) to represent HepG2 cell membrane. Silver atom (Ag^0) and silver ion (Ag^+) are used as silver models to represent possible point-to-point interaction and the effect of silver ion (Ag^+) leakage. The results show that exposure of POPC to silver ion (Ag^+) at a high concentration can cause structural conformational changes from being originally bent to straight conformation. In addition, the interaction between silver ion (Ag^+) and the lipids can cause significant amount of charge transfer that ranges from 0.14 to 0.16 for POPC and 0.12 to 0.14 for POPE. Moreover, though silver ion (Ag^+) binds three to five times stronger to the lipids than silver atom (Ag^0), both interactions are Van der Waals interaction. Finally, the presence of silver atom (Ag^0) in the lipids can be detected using UV-Vis spectrophotometer by occurrence of a red shift which is seen at 376 nm and 372 nm for POPC and POPE respectively. However, detecting silver ion (Ag^+) using this method is not feasible as no apparent shifts are shown.

* To whom correspondence should be addressed. E-mail: lwang@chem.siu.edu. Phone: (618)4536476.

1. Introduction

The utilization of silver is continually increasing. The world's demand distribution of silver in 2010 is 20% for jewelry and silverware, 7% for photography, 27% for investment and 46% for industries according to the Silver Institute.[1] The industrial application of silver has been expanding and comes in the form of silver compounds and silver nanoparticles. Silver nanoparticle industry is widely emerging[2-3] and is increasingly becoming part of our daily lives. This nanomaterial is present in cosmetics, textiles, food packaging, drug delivery systems, therapeutics, electronics, and others.[4-8] Size ranges from 1 nm to 100nm[9] and it comes in different shapes such as triangular, hexagonal, polyhedrons and others that are readily available.[10] Silver is generally low in toxicity.[4] However, when decreased to nanoscale size, this material is considered to be toxic.[11] This type of silver material is now one of the fastest growing nanomaterial industry with wide range of applications.[2-3] It is present in topical wound dressings, cosmetics, textiles, detergent, food packaging, and many consumer products we use daily.[4-8] The growth in the usage of silver is often attributed to its anti-microbial properties.[12-19] Despite the growing applications of this material, information about its toxicity is still lacking.[3, 7, 20-22] Different stabilizers or protective agents such as citrate, tannic acid, PVP(polyvinyl pyrrolidone), DDT(1-dodecanethiol), and many other are used for silver nanoparticles depending on the purpose.[23-24] The popularity of usage of this material is attributed to its antimicrobial properties,[12-17] good optical, conductive and other outstanding physical properties.[8]

Despite the growing application of silver nanoparticles,[16-17, 25-28] information about its toxicity is still lacking.[3, 7-8, 12, 20, 22, 29-41] There are some studies on silver nanoparticles that account its toxicity to its size, shape, composition and dosage.[21, 42] Others account toxicity to the surface charge[8] and possible leakage of silver ions (Ag^{+}).[42] Several studies about toxicity of

silver nanoparticle are available. However, its toxicity mechanism in the body is not fully known.[22]

Absorption in the body is through inhalation, ingestion or topical application.[4] When silver is absorbed in the body, the target organ for accumulation is the liver.[2, 43] Liver is a vital organ responsible for metabolism and detoxification in the body. In vitro studies of the liver often use HepG2 cell line which is widely accepted as a valuable and informative model system for studying human liver cells function.[22] The major lipid components of this cells are 1-palmitoyl-2-oleoyl-sn-glycero-3-phosphocholine (POPC) and 1-palmitoyl-2-oleoyI-sn-glycero-3-phosphoethanolamine (POPE).[3, 41, 44] These two lipids both have a hydrophobic tail (oleic acid, palmitic acid and part of glycerol) and a hydrophilic head containing a choline or ethanol amine group with a phosphate group which is more likely to interact with silver. In a study done by Leekumjorn, S. et. al. HepG2 cells were modeled using POPC and POPE in their lipid bilayer model. In our calculations, our model HepG2 is represented by one POPC head (phosphocholine section) and one POPE head (phosphoethanolamine section) (See Fig.1) and our silver models are silver ion (Ag^+) and silver atom (Ag^0). (Ag^+) and (Ag^0) are used to model point to point interaction of silver and a lipid. A study by Kittler, S. et. al. shows that (Ag^+) leaks out of nano-silver during storage.[22] Using (Ag^+) as model can also represent this phenomena. A 1:1 ratio of phospholipid to silver which translates to a high silver concentration is used in our interaction models. Adverse effects of exposure of model HepG2 to a highly concentrated silver model is then observed in the theoretical level. The focus of this study is on the effects of silver on the cell membrane of HepG2 cells and on a possible detection method for its presence. As such, we performed DFT and TDDFT calculations to determine the interaction strength that occur between silver and the major lipids present in HepG2 cell membrane.

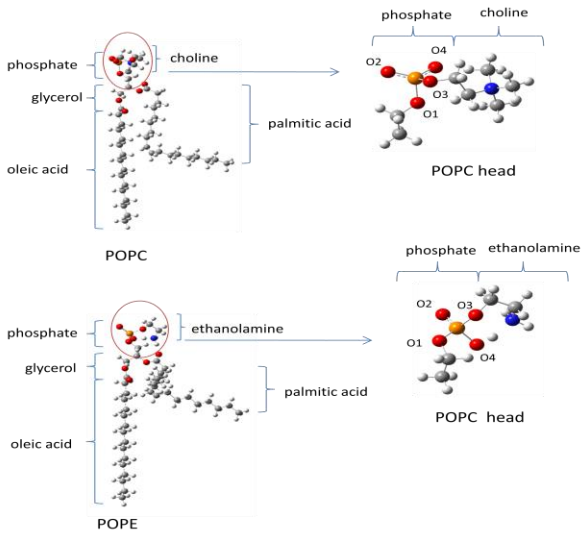

Fig 1. The model membrane of HepG2.

2. Computational details

Density Functional Theory (DFT) implemented in Gaussian 03W was used in all our calculations of geometries and Time Dependent Density Functional Theory (TDDFT) was used in our calculations of electronic properties and exited states. GaussView 3.0 was used to visualize geometries and interaction between silver and model lipids and Gauss Sum was used to generate UV-vis absorption spectra from TDDFT calculations. B3LYP functional was used together with two basis sets namely LANL2DZ for silver and 6-311+G(d,p) for the model lipids. The solvent used in all calculation is water. All convergence criteria are the same as the previous calculations.[45-51]

Interaction between metal and ligands is important research topic as it is critical to the structural property,[52] polarizability,[53] and functions.[54-57] To represent the interaction of silver and lipids present in HepG2 cells, we modeled silver using silver ion (Ag^+) and silver atom (Ag^0), and lipids using one POPC head (phosphocholine section) and one POPE head (phosphoethanolamine section). A 1:1 ratio of phospholipid to silver was used to model exposure of the cell to a high concentration of silver.

Silver models were placed at different locations around the phosphate group of model lipids to determine binding properties and possible structural changes. We chose the two major lipid constituents of HepG2 cells which are 1-palmitoyl-2-oleoyl-sn-glycero-3-phosphocholine (POPC) and 1-palmitoyl-2-oleoyI-sn-glycero-3-phosphoethanolamine (POPE) to represent HepG2 cell membrane.[41, 58] A total of sixteen (16) interaction models are established. Four (4) different positions around the phosphate group are used for silver ion-POPC head, silver ion-POPE head, silver atom-POPC head and silver atom-POPE head. Each of these four positions is modeled where the silver is near one of the oxygen present in the phosphate group. The P1, P2, P3 and P4 positions represents which closest oxygen the silver was originally located. See Figs. 2-5.

All established interaction models were inspected for structural conformational changes, possible charge transfer and binding energies are determined as well. The presence of silver in the lipid models was detected by TDDFT calculations of electronic properties and excited states of the model HepG2, and most stable interactions between silver and model lipids are followed by the generation of UV-Vis absorption spectra using Gauss Sum which shows the differences of absorption wavelength of lipids with and without silver.

3. Results

3.1 Effect of silver atom on the structure of model HepG2

The presence silver ion causes structural conformational changes to POPC head. The interaction of silver ion-POPC shown in Fig 2, results in an alteration of the alignment of phosphocholine group from being bent (see Fig 1) in the absence of silver to straight. In silver ion-POPC interaction represented in Fig 2, the silver ion's preferred positions is ranked as

P4>P1>P3>P2, where the first two has both straight conformation. The shortest distance of silver ion to the phosphate group of POPC ranges from 2.275Å to 2.281Å, where silver ion is interacting with one of freely binding oxygen of the phosphate group (O2 and O4 in Fig 2). Interaction between silver ion and POPC was observed to have a significant amount of charge transfer ranging from 0.141 to 0.164.

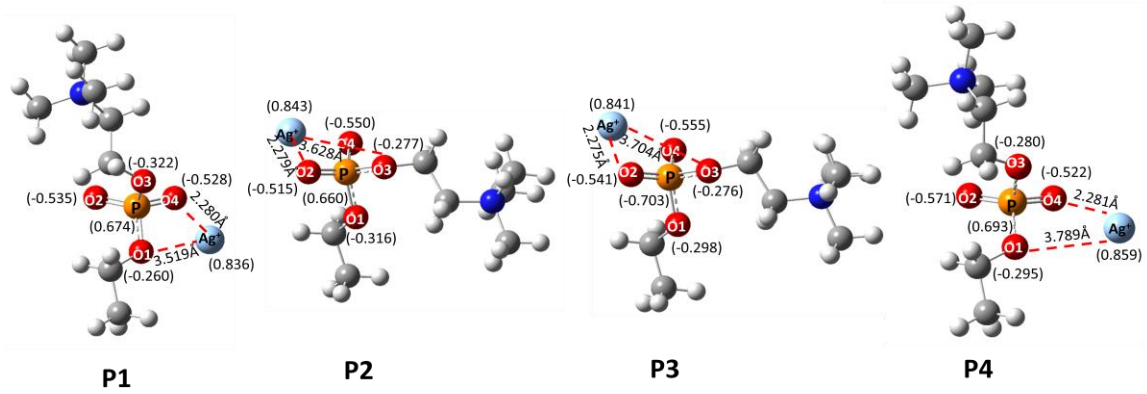

Fig 2. Silver ion-POPC head interaction, distances and Mulliken atomic charges, the red, orange, gray white, royal blue and light blue balls represent oxygen, phosphorus, carbon, hydrogen, nitrogen, and silver.

For the silver atom-POPC interaction shown in Fig 3, the preferred position of the silver atom is P3>P1>P2>P4 with bent-straight-bent-straight conformation pattern. The shortest distance observed between the silver atom and phosphate group of POPC is 4.72 Å (P4) which is about twice the distance of silver ion-POPC interaction. This indicates the attraction between the silver and the phosphate of POPC weaker when silver is in atomic form. Silver atom-POPC interaction was observed to have charge transfer of 0.004-0.012 which is considerably small.

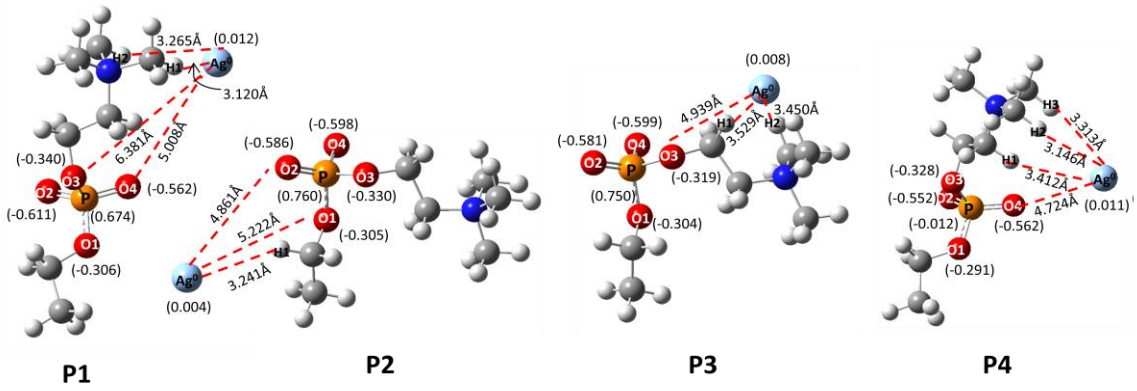

Fig 3. Silver atom-POPC head interaction, distances and Mulliken atomic charges, the red, orange, gray white, royal blue and light blue balls represent oxygen, phosphorus, carbon, hydrogen, nitrogen and silver.

For the POPE-silver ion interaction in Fig 4, it was observed that the POPE was likely to have a bent conformation which is the same without being exposed to silver ion. The silver ion preference is ranked as P4>P3>P1>P2 where all four has a bent conformation which is the same as original. The shortest distance of silver ion to the phosphate of POPE is 2.29 Å (P1, P3, P4 of Fig 4) which is very similar to silver ion-POPC shortest distance of 2.28 Å. POPE-silver ion was observed to have a significant charge transfer that ranges from 0.124 to 0.137.

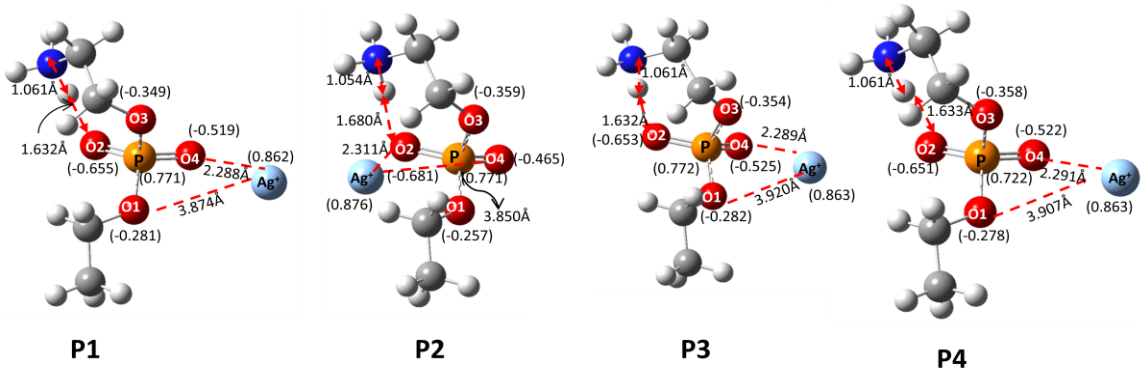

Fig 4. Silver ion-POPE head interaction, distances and Mulliken atomic charges, the red, orange, gray white, royal blue and light blue balls represent oxygen, phosphorus, carbon, hydrogen, nitrogen and silver.

For the POPE-silver atom interaction in Fig 5, structural conformation change was not observed. The silver atom preference around POPE is P3>P4>P1>P2. The distance between the

phosphate group of POPE and silver atom ranges from 4.89Å to 5.26Å which is about twice of the silver ion-POPE distance. It was observed that weaker attraction occur in the presence of silver atom in POPE. In addition, an insignificant amount of charge transfer that ranges from 0.005-0.009 occurs in the silver atom-POPE interaction.

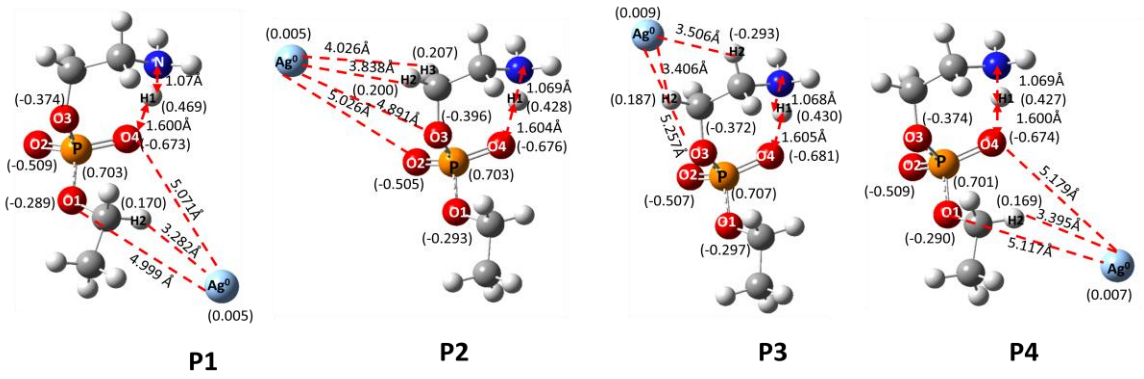

Fig 5. Silver atom- POPE head interaction distances and Mulliken atomic charges, the red, orange, gray white, royal blue and light blue balls represent oxygen, phosphorus, carbon, hydrogen, nitrogen and silver.

Structural conformation change is not observed in POPE upon exposure to either silver ion (Fig 4) or silver atom (Fig 5). This means that POPE is not subject to structural conformational change at high concentration of silver.

In all four sets models, only silver-ion POPC model results in a structural conformational change from being originally bent to a straight conformation. Furthermore, the attraction between silver and lipid is stronger when silver is in the form of silver ion. This is confirmed by a shorter distance between silver ion and the phosphate groups of the lipids. This stronger attraction with silver ion is also preceded by a significant amount of charge transfer which ranges from 0.141 to 0.164 for POPC and 0.124 to 0.137 for POPE.

3.2 Binding Energies of interaction between silver and lipids present in HepG2 cells

Binding energies of silver to lipid models were obtained. Table 1 and Table 2 show the binding energies of silver ion and silver atom with POPC and POPE respectively.

Table 1. Binding energies of POPC with silver

Position #	Binding Energy with **Silver ion** (kcal/ mol)	Binding Energy with **Silver atom** (kcal/ mol)
P1	-5.84	-1.83
P2	-5.16	-1.70
P3	-5.74	-2.24
P4	-7.30	-1.48

Table 2. Binding energies of POPE with silver

Position #	Binding Energy with **Silver ion** (kcal/ mol)	Binding Energy with **Silver atom** (kcal/ mol)
P1	-4.84	-1.70
P2	-3.38	-1.45
P3	-4.91	-1.94
P4	-4.92	-1.72

All calculated binding interactions are exothermic. Moreover, it was observed that binding energy of POPC and POPE with the silver ion is three to five times greater than with the silver atom. This indicates a stronger binding interaction between the lipids and silver ion which is also confirmed by a shorter distance of 2.28 Å-2.29 Å as previously mentioned. Similarly, this

means that desorption of silver atom from model lipids will be easier than silver ion. In terms of possible accumulation in the cell membrane the presence of silver ion will be much greater than that of silver atom if no other reaction is involve. The binding energies of between silver and the model lipids (Table1 and 2) which falls between -7.30 to -1.45 kcal/mol suggests that Van der Waals intermolecular interaction exists.

3.3 UV Vis spectra, band gaps and molecular orbitals of interacting silver-model lipids present in HepG2 cells

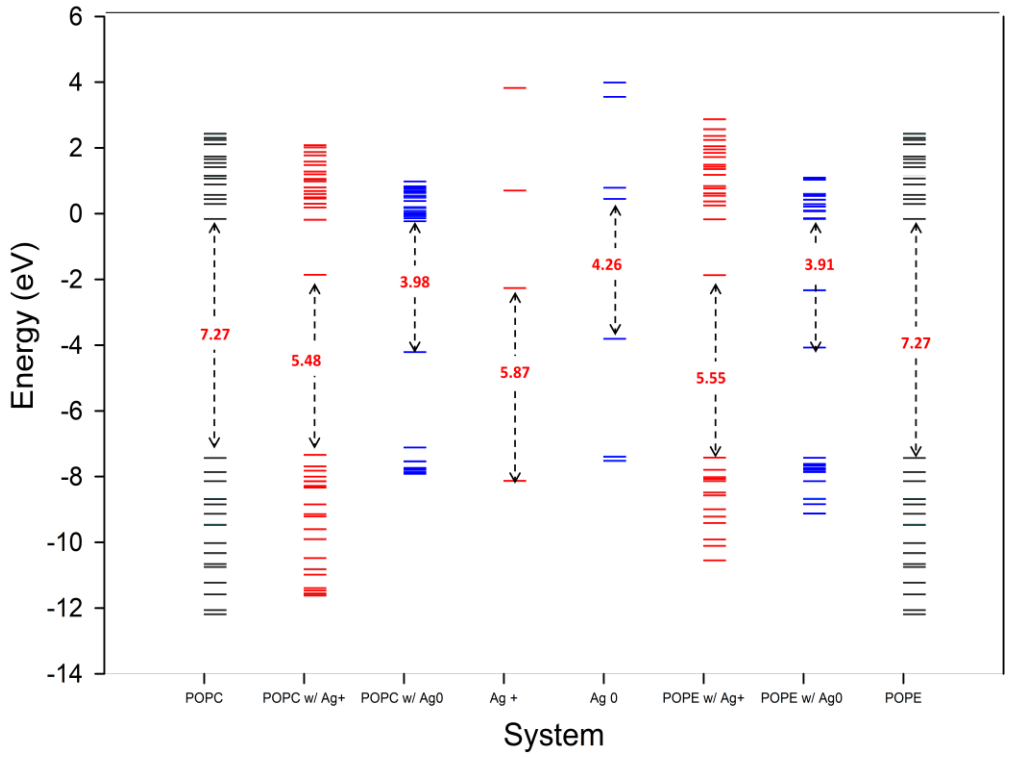

Fig 6. Energy diagram obtained from DFT calculations.

An energy diagram of silver ion, silver atom, POPC and POPE heads and their exposure to silver atom or silver ion is shown in Fig 6. POPC and POPE head (black in Fig. 6) takes the same amount of excitation energy from HOMO to LUMO (7.27 eV). The presence of silver either in ionic or atomic form in these two lipids increases their reactivity. In the interaction with

silver ion (red in Fig 6), the HOMO resembles that of the two lipids while the LUMO resembles that of the silver ion (Ag+) decreasing the excitation energy by a fourth of that of the lipids, 1.77 eV to 1.79 eV for POPE and POPC respectively. The HOMO-LUMO excitation energy values of 5.48 eV for *POPC w/ Ag+* and 5.55 eV for *POPE w/ Ag+* is more likely influenced by the silver ion which has a very similar HOMO-LUMO band gap of 5.87 eV.

In the silver atom-lipid interaction, (blue in Fig 6) the HOMO resembles that of the silver atom and the LUMO resembles that of the two lipids which also decreases the excitation energy of the two lipids by about half of that of the lipids, 3.29 eV to 3.36 eV for POPC and POPE respectively. The HOMO-LUMO excitation energy values of 3.98 eV for *POPC w/ Ag0* and 3.91 eV for *POPE w/ Ag0* is influenced by the presence of the silver atom with a HOMO-LUMO band gap of 4.26 eV.

UV-Vis spectra are generated to further understand the effects of silver to the model lipids. Fig 6 and Fig 7 show the absorption spectra of silver atom (gray), POPC head and POPE head respectively (red), and their exposure to silver ion (blue) and silver atom (green). TDDFT calculations for silver ion results in the absence of visible peak, thus absorption spectra for silver ion cannot be generated. The peak values are available in Tables 4, 6, 8, 10, 12, 14 and 16.

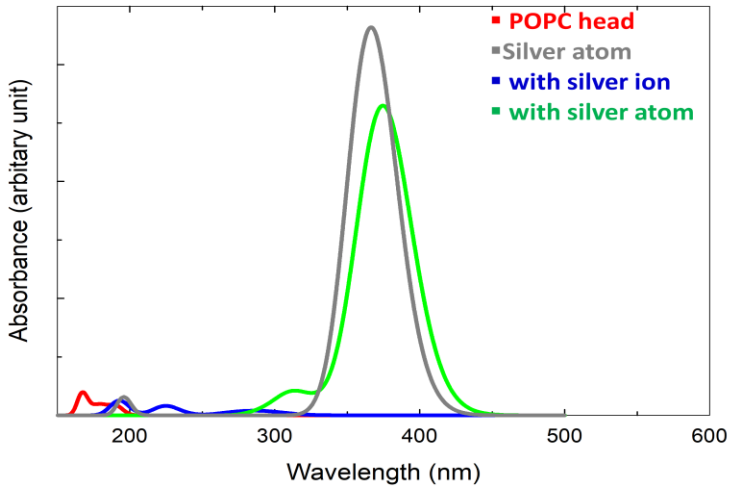

Fig 7. Absorption spectra of POPC with silver.

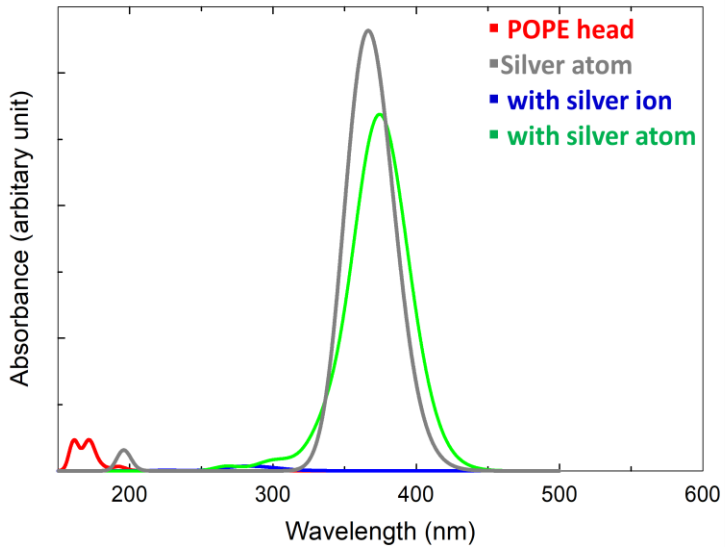

Fig 8. Absorption spectra of POPE with silver

The presence of both silver ion and silver atom in POPC and POPE both yielded a red shift. However, only POPC and POPE exposure to silver atom (green) , which are seen in 376 nm and 372 nm respectively, results with the greatest red shift of more intensified absorption that is observable near the visible light region. . This peak intensity at the wavelengths mentioned is definitely influenced by the presence of silver atom which is observed at 366 nm (gray). Experimental value of absorbance of atomic silver for silver nanoparticles with size of <10nm is 385 nm.[59] Our silver model are < 1nm size and has a difference of 2.34%-3.38% from experimental results Exposure of POPC and POPE to silver ion (blue) can be represented by a red shift less than that of the silver atom with a weaker intensity of absorption but can be difficult to detect in the UV region. These results suggests that this often used spectroscopy method can be used to detect the presence of silver atom in lipids present in HepG2 cell membrane. However, the presence of silver ion will not be possible for this spectroscopy method.

Table 3. Molecular Orbital and corresponding energies of POPC head

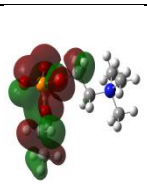	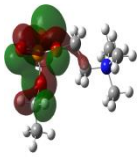	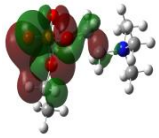	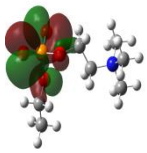	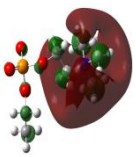	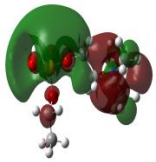	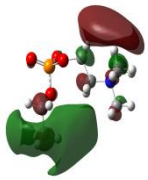	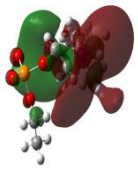	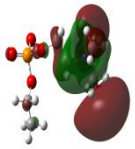
MO 54	MO 55	MO 56	MO 57	MO 58	MO 59	MO 60	MO 61	MO 62
(HOMO-3)	(HOMO-2)	(HOMO-1)	(HOMO)	(LUMO)	(LUMO+1)	(LUMO+2)	(LUMO+3)	(LUMO+4)
-8.41 eV	-7.78 eV	-7.65 eV	-7.40 eV	-0.22 eV	0.03 eV	0.25 eV	0.41 eV	0.49 eV

Table 4. Calculated Excitation Energies, Oscillator Strengths and Molecular Orbitals(MOs)of POPC head

Compound	Energy (eV)	Wavelength	Oscillator Strength	MOs	Coefficient
POPC head	6.51	191 nm	0.0205	57->58	0.48867
				57->59	0.47521
				57->61	0.10978
	6.96	178 nm	0.0128	55->59	0.23581
				56->58	0.41715
				56->59	0.48575
	7.44	167 nm	0.0277	54->58	0.22421
				54->59	0.13976
				55->60	0.54131
				55->61	0.21345
				56->60	0.17852
				57->62	0.14156

Looking at the molecular orbitals that participate in the excitation of POPC, POPE and their exposure to silver ion and atom (Table 3-14) will give insights of their characteristics and interactions. Table 3 shows the shape of the MOs (Table 4) that participate in excitation of POPC. When excited from HOMO (MO 57) to LUMO (MO 58), the electron density in POPC head shifts from the phosphate group to the choline group of the head.

Table 5. Molecular orbital and corresponding energies of POPC head exposed to silver ion (Ag^+)

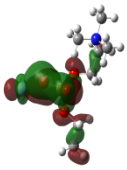	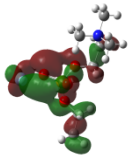	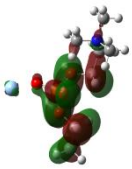	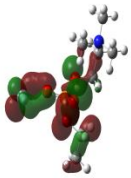	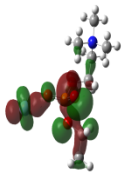	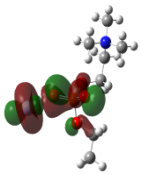	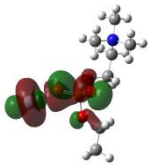	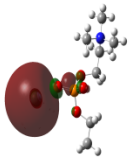
MO 56 (HOMO-6) -9.20 eV	MO 57 (HOMO-5) -9.14 eV	MO 58 (HOMO-4) -8.84 eV	MO 59 (HOMO-3) -8.33 eV	MO 60 (HOMO-2) -8.27 eV	MO 65 (HOMO-1) -7.67 eV	MO 66 (HOMO) -7.32 eV	MO 67 (LUMO) -1.85 eV

Table 6. Calculated excitation energies, oscillator strengths and frontier molecular orbitals(MOs)of POPC head exposed to silver ion(Ag^+)

Compound	Energy (eV)	Wavelength	Oscillator Strength	MOs	Coefficient
POPC head with silver ion	4.22	294 nm	0.0102	60->67 56->67	0.16803 0.65378
	5.48	226 nm	0.0198	56->67 59->67 60->67 65->67 66->67	0.12509 0.46516 0.40858 0.21029 0.16455
	6.42	193 nm	0.0276	56->67 57->67 58->67 60->67	0.32254 0.48223 0.35562 0.11183

Upon exposure of POPC to silver ion (Table 5), the electron density in the HOMO (MO 66) concentrates in phosphate group sharing some with the silver ion (Ag^+). This shape of HOMO has more similarities to the HOMO (MO 58) of POPC in Table 3. When excited to LUMO (MO 67) the majority of electron density shifts to the silver ion (Ag^+).

Table 7. Molecular orbital and corresponding energies of POPC head exposed to silver atom (Ag^0)

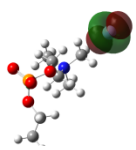	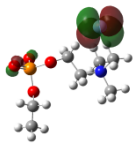	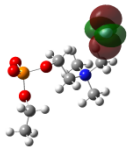	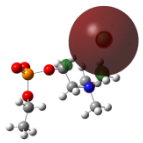	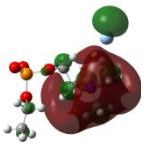	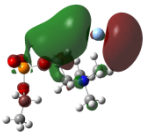	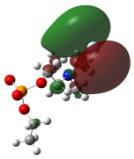	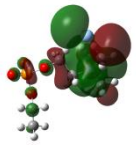	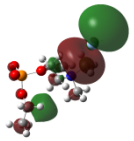
MO 60	MO 61	MO 62	MO 67	MO 68	MO 69	MO 70	MO 71	MO72
(HOMO-7)	(HOMO-6)	(HOMO-5)	(HOMO)	(LUMO)	(LUMO+1)	(LUMO+2)	(LUMO+3)	(LUMO+4)
			-4.14eV(α)	-0.22eV(α)	-0.027eV(α)	0(α)	-0.19eV(α)	-0.19eV(α)
-7.73eV(β)	-7.73eV(β)	-7.70 eV(β)	-2.37eV(β)					

Table 8. Calculated excitation energies, oscillator strengths and molecular orbitals(MOs) of POPC head exposed to silver atom (Ag^0)

Compound	Energy (eV)	Wavelength	Oscillator Strength	MOs	Coefficient
POPC with	3.27	379 nm	0.2375	67A->68A	0.85687
				67A->69A	0.17413
				67A->70A	0.13307
				67A->71A	0.21269
				67A->72A	0.37783
				60B-> 67B	0.11186
silver atom	3.30	376 nm	0.2596	67A->68A	0.13994
				67A->69A	0.89970
				67A->70A	0.10024
				67A->71A	0.28576
				67A->72A	0.21025
				61B->67B	0.11592
(Ag^0)	3.31	375 nm	0.2189	67A->68A	0.12688
				67A->70A	0.95985
				67A->72A	0.11964
				67A->73A	0.13624
				62B->67B	0.12400

When silver atom (Ag^0) is present instead of silver ion around POPC (Table 7), the electron density in the HOMO (MO 67) is concentrated in the silver atom, similar to the LUMO (MO 67) of POPC with silver ion in Table 5. When excited to LUMO (MO 68), the electron density shifts to the choline group of POPC head sharing some with silver atom. This LUMO (MO 68) of POPC with silver atom is similar to the LUMO of just POPC alone in Table 3.

Table 9. Molecular Orbital and corresponding energies of POPE head

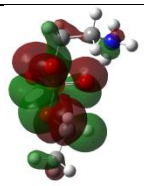	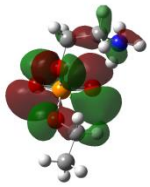	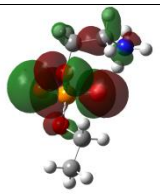	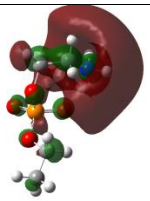	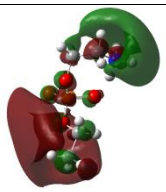	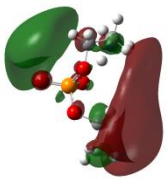	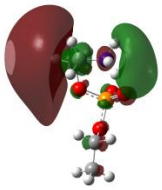
MO 43	MO 44	MO 45	MO 46	MO 47	MO 48	MO 49
(HOMO-2)	(HOMO-1)	(HOMO)	(LUMO)	(LUMO+1)	(LUMO+2)	(LUMO+3)
-8.14 eV	-7.86 eV	-7.43 eV	-0.14 eV	0.27 eV	0.44 eV	0.54 eV

Table 10. Calculated excitation energies, oscillator strengths and molecular orbitals(MOs) of POPE head

Compound	Energy (eV)	Wavelength	Oscillator Strength	MOs	Coefficient
POPE head	7.21	172 nm	0.0449	43>46	0.63842
				43->47	0.18874
				44->48	0.11000
				45->47	0.10847
	7.29	170 nm	0.0143	45->49	0.69215
	7.73	160 nm	0.0438	42->46	0.29000
				43->46	0.11809
				43->47	0.24401
				43->48	0.28259
				44->49	0.46684

In the excitation of POPE, the electron density which is concentrated in the phosphate group in the HOMO (MO 45) shifts to the ethanol amine group upon excitation to the LUMO (MO 46) shown in Table 9. In the exposure of POPE to silver ion the electron density is shared between the phosphate group and silver ion in the HOMO (MO 54) shown in Table 11. Upon excitation to LUMO (MO 55) the electron density concentration shifts to the silver ion. This mechanism is very similar POPC exposure to silver ion.

Table 11. Molecular orbital and corresponding energies of POPE head exposed to silver ion (Ag^+)

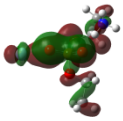	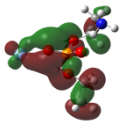	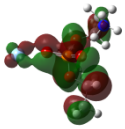	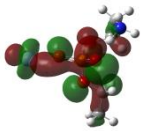	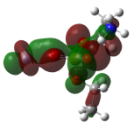	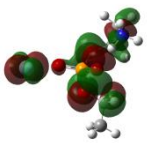	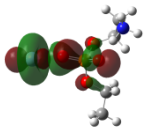	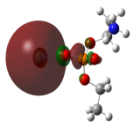
MO 44	MO 45	MO 46	MO 47	MO 48	MO 51	MO 54	MO 55
(HOMO-10)	(HOMO-9)	(HOMO-8)	(HOMO-7)	HOMO-6)	(HOMO-3)	(HOMO)	(LUMO)
-9.39 eV	-9.20 eV	-8.98 eV	-8.54 eV	-8.46 eV	-8.05 eV	-7.40 eV	-1.85 eV

Table12. Calculated excitation energies, oscillator strengths and molecular orbitals(MOs) of POPE head exposed to silver ion(Ag^+)

Compound	Energy (eV)	Wavelength	Oscillator Strength	MOs	Coefficient
POPE head with silver ion (Ag^+)	5.76	215 nm	0.0201	48->55 51->55 54->55	0.61398 0.26652 0.10543
	5.84	212 nm	0.0286	45->55 46->55 47->55 54->55	0.14726 0.10009 0.64492 0.11872
	6.60	188 nm	0.0109	44->55 45->55	0.19674 0.55823

	46->55	0.35031
	47->55	0.11517

In the presence of silver atom in POPE seen in Table 13, the electron density is concentrated around the silver atom in the HOMO (MO 55). Upon excitation to LUMO (MO 56), the electron density shifts to the ethanol amine group sharing a little with the silver.

Table 13. Molecular orbital and corresponding energies of POPE head exposed to silver atom (Ag^0)

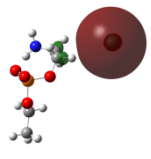	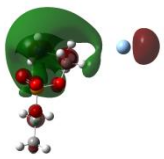	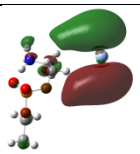	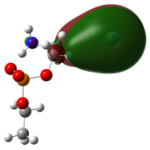	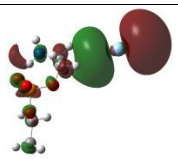	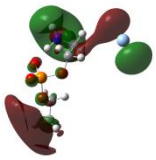	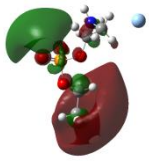
MO 55 (HOMO)	MO 56 (LUMO)	MO 57 (LUMO+1)	MO 58 (LUMO+2)	MO 59 (LUMO+3)	MO 60 (LUMO+4)	MO 61 (LUMO+5)
-4.05eV(α)	-0.14eV(α)	0.05eV(α)	0.08eV(α)	0.19eV(α)	0.41eV(α)	0.52eV(α)

Table14. Calculated excitation energies, oscillator strengths and molecular orbitals(MOs) of POPE head exposed to silver atom (Ag^0)

Compound	Energy (eV)	Wavelength	Oscillator Strength	MOs	Coefficient
POPE head with silver	3.25	381 nm	0.2485	55A->56A 55A->57A 55A->59A 55A->60A	0.85197 0.18608 0.46118 0.10142
atom(Ag^+)	3.33	373 nm	0.2474	55A->57A 55A->58A 55A->59A 55A->61A	0.71435 0.64253 0.17332 0.13114

3.34	372 nm	0.2536	55A->57A 55A->58A 55A->59A 55A->60A	0.60355 0.73294 0.18764 0.20018

Table 15. Molecular orbital and corresponding energies of silver atom (Ag^0)

	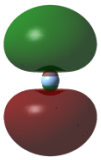	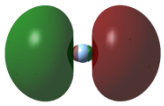	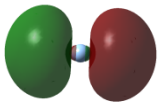
MO 10 (HOMO) 3.78 eV	MO 11 (LUMO+1) 0.44 eV	MO 12 (LUMO+2) 0.44 eV	MO 13 (LUMO+3) 0.44 eV

Table 16. Calculated excitation energies, oscillator strengths and molecular orbitals (MOs) of silver atom (Ag^0)

Compound	Energy (eV)	Wavelength	Oscillator Strength	MOs	Coefficient
Silver atom (Ag^0)	3.3848	366 nm	0.3054	10A->11A 10A->13A	0.98740 0.14880
	3.3848	366 nm	0.3054	10A->11A 10A->13A	0.14883 0.98738
	3.3848	366 nm	0.3054	10A->12A	0.99853

Overall, the molecular orbitals of POPC and POPE upon excitation from HOMO to LUMO share the similar mechanism where the electron density shifts from the phosphate group to the choline or ethanol amine group. The exposure of these two lipids to silver ion and silver atom also share similar mechanism upon excitation. In the presence of silver ion in both lipids,

electron density shifts from being shared between the silver ion and phosphate group to the silver ion upon excitation from HOMO to LUMO. In the presence of silver atom in both lipids, the electron density shifts from the silver atom to the choline group or ethanol amine group sharing a little to the silver atom. We mention that the results are at the single molecule level and effect of aggregation may also be interested in the experimental observations[60] and is important to consider in future studies. Similarly, single Ag atom or ion is different from nanoparticles,[61-67] which have different properties. Nevertheless, the DFT results can serve as an important input to build force field for dynamics simulations[68-69] that are necessary for a better understanding of the processes.

4. Conclusions

To sum up, we have obtained four major results from modeling the interaction of silver with lipids present in HepG2 cells. First, a very high concentration of silver ion introduced in POPC lipid can produce a structural conformation change in the POPC head part of from being originally bent to being straight conformation. Second, the presence of silver ion in the model lipids results in a significant charge transfer ranging from 0.141 to 0.164 for POPC and 0.124 to 0.137 for POPE. Third, the binding interaction between silver ion and the lipids is found to be greater with silver atom. The interaction between silver and the lipids is categorized as Van der Waals intermolecular interaction. Lastly, the presence of silver in the lipids can be detected through UV-vis spectrophotometer. A UV-vis absorption spectra were generated and a red shift was observed in the presence of silver in the lipids. A greater red shift within the visible light region and a more intense absorption were observed when the lipids are exposed to silver atom. Exposure to silver atom was observed in the UV light region with a very low intensity. This

indicates that this using spectrometry for detection of the presence of silver atom in the model lipids is possible but will be difficult for detection of silver ion.

Acknowledgment

We thank Christian Mason for performing some calculations. This work was partly supported by the National Science Foundation (NSF-CBET-0709113).

References

1. Klapwijck, P., The Silver Market in 2011. *Silver Institute, Nov. 16*, **2011**, p.9.
2. Cho, J. H.; Kulkarni, A.; Kim, H.; Yoon, J. U.; Sung, J. H.; Yu, I. J.; Kim, T., Numerical Study on Spatial Distribution of Silver Nanoparticles inside Whole-Body Type Inhalation Toxicity Chamber. *J. Mech. Sci. Tech.* **2010**, *24*, 2215-2220.
3. Ahmed, M.; Posgai, R.; Gorey, T. J.; Nielsen, M.; Hussain, S. M.; Rowe, J. J., Silver Nanoparticles Induced Heat Shock Protein 70, Oxidative Stress and Apoptosis in Drosophilia Melanogaster. *Toxicol. App. Pharma.* **2009**, *242*, 263-269.
4. Merrill, J. C.; Morton, J. J. P.; Solleau, S. D., Metals. In *Principles and Methods of Toxicology*, Hayes, A. W., Ed. Taylor & Francis Group: Boca Raton, 2008; p 867.
5. Li, M.; Al-Jamal, K. T.; Kostarelos, K.; Reineke, J., Review: Physiologically Based Pharmacokinetic Modelling of Nanoparticles. *ACS Nano* **2010**, *4*, 6303-6317.
6. Lu, W.; Senapati, D.; Wang, S.; Tovmachenko, O.; Singh, A. K.; Yu, H.; Ray, P. C., Effect of Surface Coating on the Toxicity of Silver Nanomaterials on Human Skin Keratinocytes. *Chem. Phys. Lett.* **2010**, *487*, 92-96.
7. Asha Rani, P. V.; Low Kah Mun, G.; Hande, M. P.; Valiyaveettil, S., Cytotoxicity and Genotoxicity of Silver Nanoparticles in Human Cells. *ACS Nano* **2009**, *3*, 279-290.
8. El Badawy, A. M.; Silva, R. G.; Morris, B.; Scheckel, K. G.; Suidan, M.; Tolaymat., T. M., Surface Charge-Dependent Toxicity of Silver Nanoparticles. *Environ. Sci. Technol.* **2011**, *45*, 283-287.
9. Sanvicens, N.; Marco, M. P., Review: Multifunctional Nanoparticles-Properties and Prospects for Their Use in Human Medicine. *Trends Biotechnol.* **2008**, *8*, 425-433.
10. Yang, Y.; Matsubara, S.; Xiong, L.; Hayakawa, T.; Nogami, M., Solvothermal Synthesis of Multiple Shapes of Silver Nanoparticle and Their Sers Properties. *J. Phys. Chem. C* **2007**, *111*, 9095-9104.
11. Protection, E., Groups Petition Epa for Action on Nano-Silver. **2008**.
12. Sondi, I.; Salopek-Sondi, B., Silver Nanoparticles as Antimicrobial Agent: A Case Study on E. Coli as a Model for Gram-Negative Bacteria. *J. Colloid Interface Sci.* **2004**, *275*, 177-182.
13. Uygun, M.; Kahveci, M. U.; Odaci, D.; Tumur, S.; Yagci, Y., Antibacterial Acrylamide Hydrogels Containing Silver Nanoparticles by Simultaneous Photoinduced Free Radical Polymerization and Electron Transfer Processes. Macromol. *Chem. Phys.* **2009**, *210*, 1867-1875.

14. Singh, M.; Singh, S.; Prasad, S.; Gambhir, I. S., Nanotechnology in Medicine and Antibacterial Effect of Silver Nanoparticles. *Dig. J. Nanomater. Biostructures* **2008**, *3*, 115-122.
15. Lok, C. N.; Ho, C. M.; Chen, R.; He, Q. Y.; Yu, W. Y.; Sun, H.; Tam, P. K.; Chiu, J. F.; Che, C. M., Proteomic Analysis of the Mode of Antibacterial Action of Silver Nanoparticles. *J. Proteome Res.* **2006**, *5*, 916-924.
16. Gogoi, S. K.; Gopinath, P.; Paul, A.; Ramesh, A.; Ghosh, S. S.; Chattopadhyay, A., Green Fluorescent Protein-Expressing Escherichia Coli as a Model System for Investigating the Antimicrobial Activities of Silver Nanoparticles. *Langmuir* **2006**, *22*, 9322-9328.
17. Kim, J. S.; Kuk, E.; Yu, K. N.; Kim, J. H.; Park, S. J.; Lee, H. J.; Kim, S. H.; Park, Y. K.; Park, Y. H.; Hwang, C. Y., Antimicrobial Effects of Silver Nanoparticles. *Nanomedicine* **2007**, *3*, 95-101.
18. Tortella, G. R.; Pieretti, J. C.; Rubilar, O.; Fernandez-Baldo, M.; Benavides-Mendoza, A.; Dieza, M. C.; Seabra, A. B., Silver, Copper and Copper Oxide Nanoparticles in the Fight against Human Viruses: Progress and Perspectives. *Critical Rev. Biotechnol.* **2022**, *42*, 431-449.
19. Akintelu, S. A.; Olugbeko, S. C.; Folorunso, A. S.; Oyebamiji, A. K.; Folorunso, F. A., Potentials of Phytosynthesized Silver Nanoparticles in Biomedical Fields: A Review. *Int. Nano Lett.* **2021**, *11*, 273-293.
20. Garza-Ocañas, L.; Ferrer, D. A.; Burt, J.; Diaz-Torres, L. A.; Cabrera, M. R.; Rodriguez, V. T.; Rangel, R. L.; Romanovicz, D.; Jose-Yacaman, M., Biodistribution and Long Term Fate of Silver Nanoparticles Functionalized with Bovine Serum Albumin in Rats. *Metallomics* **2009**, *2*, 204-210
21. Kawata, K.; Osawa, M.; Okabe, S., In Vitro Toxicity of Silver Nanoparticles at Noncytotoxic Doses to Hepg2 Human Hepatoma Cells. *Envi. Sci. Technol.* **2009**, *43*, 6046-6051.
22. Kramer, J.; Bell, R.; Smith, S.; Gorsuch, J., Silver Nanoparticle Toxicity and Biocides: Need for Chemical Speciation. *Integr. Environ. Asses. Manag.* **2009**, *4*, 720-722.
23. Mo, L.; Liu, D.; Li, W.; Li, L.; Wang, L.; Zhou, X., Effects of Dodecylamine and Dodecanethiol on the Conductive Properties of Nano-Ag Films. *Appl. Surf. Sci.* **2011**, *257*, 5746-5753.
24. Nel, A. E.; Mädler, L.; Velegol, D.; Xia, T.; Hoek, E. M. V.; Somasundaran, P.; Klaessig, F.; Castranova, V.; Thompson, M., Understanding Biophysicochemical Interactions at the Nano–Bio Interface. *Nat. Mater.* **2009**, *8*, 543-557.
25. Bhardwaj, A. K.; Sundaram, S.; Yadav, K. K.; Srivastav, A. L., An Overview of Silver Nano-Particles as Promising Materials for Water Disinfection. *Environ. Technol. Innov.* **2021**, *23*, 10721.
26. Ahmed, H. M.; Roy, A.; Wahab, M.; Ahmed, M.; Othman-Qadir, G.; Elesawy, B. H.; Khandaker, M. U.; Islam, M. N.; Emran, T. B., Applications of Nanomaterials in Agrifood and Pharmaceutical Industry. *J. Nanomater.* **2021**, *2021*, 1472096.
27. Derakhshan, M. A.; Amani, A.; Faridi-Majidi, R., State-of-the-Art of Nanodiagnostics and Nanotherapeutics against Sars-Cov-2. *ACS Appl. Mater. Interfaces* **2021**, *13*, 14816-14843.
28. Kamali, M.; Khodaparast, Z., Review on Recent Developments on Pulp and Paper Mill Wastewater Treatment. *Ecotoxicology and Environmental Safety* **2015**, *114*, 326-342.

29. Rahman, A.; Sarkar, A.; Yadav, O. P.; Achari, G.; Slobodnik, J., Potential Human Health Risks Due to Environmental Exposure to Nano- and Microplastics and Knowledge Gaps: A Scoping Review. *Sci. Total Environ.* **2021**, *757*, 143872.
30. Egbuna, C., et al., Toxicity of Nanoparticles in Biomedical Application: Nanotoxicology. *J. Toxicol.* **2021**, *2021*, 9954443.
31. Tighe-Neira, R.; Gonzalez-Villagra, J.; Nunes-Nesi, A.; Inostroza-Blancheteau, C., Impact of Nanoparticles and Their Ionic Counterparts Derived from Heavy Metals on the Physiology of Food Crops. *Plant Physiol. Biochem.* **2022**, *172*, 14-23.
32. Ramzan, U., et al., New Insights for Exploring the Risks of Bioaccumulation, Molecular Mechanisms, and Cellular Toxicities of Agnps in Aquatic Ecosystem. *Water* **2022**, *14*, 2192.
33. Ferdous, Z.; Nemmar, A., Health Impact of Silver Nanoparticles: A Review of the Biodistribution and Toxicity Following Various Routes of Exposure. *Int. J. Mol. Sci.* **2020**, *21*, 2375.
34. Halsted, C. H., B-Vitamin Dependent Methionine Metabolism and Alcoholic Liver Disease. *Clinical Chemistry and Laboratory Medicine* **2013**, *51*, 457-465.
35. Stensberg, M. C.; Wei, Q.; McLamore, E. S.; Porterfield, D. M.; Wei, A.; lveda, M. S. S., Toxicological Studies on Silver Nanoparticles: Challenges and Opportunities in Assessment, Monitoring and Imaging. *Nanomedicine (Lond)* **2011**, *6*, 879-898.
36. Toro, R. G., et al., Evaluation of Long–Lasting Antibacterial Properties and Cytotoxic Behavior of Functionalized Silver-Nanocellulose Composite. *Mater.* **2021**, *14*, 4198.
37. Jaswal, T.; Gupta, J., A Review on the Toxicity of Silver Nanoparticles on Human Health. *Mater. Today: Proceedings* **2021**, https://doi.org/10.1016/j.matpr.2021.04.266.
38. Urani, C.; Melchioretto, C.; Crosta, G. F., Cytotoxicity and Induction of Protective Mechanism in Hepg2 Cells Exposed to Cadmium. *Toxicol. in Vit.* **2005**, *19*, 887-892.
39. You, M.; Crabb, D. W., Recent Advances in Alcoholic Liver Disease - Ii. Minireview: Molecular Mechanisms of Alcoholic Fatty Liver. *Am. J. Physiology-Gastrointestinal and Liver Physiol.* **2004**, *287*, G1-G6.
40. Panyala, N. R.; Peňa-Mendez, E. M.; Havel, J., Review: Silver or Silver Nanoparticles: A Hazardous Threat to the Environment and Human Health? *J. Appl. Biomed.* **2008**, *6*, 117-129.
41. Leekumjorn, S.; Wu, Y.; Sum, A. K.; Chan, C., Experimental and Computational Studies Investigating Trehalose Protection of Hepg2 Cells from Palmitate-Induced Toxicity. *Biophys J.* **2008**, *94*, 2869-2883.
42. Kittler, S.; Greulich, C.; Diendorf, J.; Koller, M.; Epple, M., Toxicity of Silver Nanoparticles Increases During Storage Because of Slow Dissolution under Release of Silver Ions. *Chem. Mater.* **2010**, *22*, 4548-4554.
43. Li, J.; Chen, C.; Xia, T., Understanding Nanomaterial–Liver Interactions to Facilitate the Development of Safer Nanoapplications. *Adv. Mater.* **2022**, *34*, 2106456.
44. She, Y.; Narindrasorask, S.; Yang, S.; Spitale, N.; Roberts, E. A.; Sarkar, B., Identification of Metal-Binding Proteins in Human Hepatoma Lines by Immobilized Metal Affinity Chromatography and Mass Spectrometry. *Mol. Cell. Biol.* **2003**, *2*, 1306-1318.
45. McCarroll, M. E.; Shi, Y.; Harris, S.; Puli, S.; Kimaru, I.; Xu, R.; Wang, L.; Dyer, D. J., Computational Prediction and Experimental Evaluation of a Photoinduced Electron-Transfer Sensor. *J. Phys. Chem. B* **2006**, *110*, 22991.

46. Walkup, L. L.; Weerasinghe, K. C.; Tao, M.; Zhou, X.; Zhang, M.; Liu, D.; Wang, L., Importance of Dynamics in Electron Excitation and Transfer of Organic Dyes. *J. Phys. Chem. C* **2010**, *114*, 19521.
47. Wang, T.; Weerasinghe, K. C.; Liu, D.; Li, W.; Yan, X.; Zhou, X.; Wang, L., Ambipolar Organic Semiconductors with Cascades of Energy Levels for Generating Long-Lived Charge Separated States: A Donor–Acceptor1–Acceptor2 Architectural Triarylamine Dye. *J. Mater. Chem. C* **2014**, *2*, 5466.
48. Zhou, X.; Liu, D.; Wang, T.; Hu, X.; Guo, J.; Weerasinghe, K. C.; Wang, L.; Li, W., Synthesis and Photophysical Studies of Triazine-Linked Porphyrin-Perylene Bismide Dyad with Long-Lived Perylene Triplet State. *J. Photochem. Photobiol. A: Chem.* **2014**, *274*, 57.
49. Wang, T., et al., Enhancing Photoinduced Charge Separation through Donor Moiety in Donor-Accepter Organic Semiconductors". *J. Phys. Chem. C* **2016**, *120*, 25263-25275.
50. Wang, W.; Lv, F.; Lei, B.; Wan, S.; Luo, M. C.; Guo, S. J., Tuning Nanowires and Nanotubes for Efficient Fuel-Cell Electrocatalysis. *Adv. Mater.* **2016**, *28*, 10117-10141.
51. Wang, T.; Weerasinghe, K. C.; Ubaldo, P. C.; Liu, D.; Li, W.; Zhou, X.; Wang, L., Tuning Electron–Hole Distance of the Excitons in Organic Moleculesusing Functional Groups. *Chem. Phys. Lett.* **2015**, *618*, 142.
52. Spivey, K.; Williams, J. I.; Wang, L., Structures of Undecagold Clusters: Ligand Effect. *Chem. Phys. Lett.* **2006**, *432*, 163-166.
53. Fan, X.; Wu, Z.; Wang, L.; Wang, C., Exploring the Origin of High Dechlorination Activity in Polar Materials $M_2b_5o_9cl$ (M= Ca, Sr, Ba, Pb) with Built-in Electric Field. *Chem. Mater.* **2017**, *29*, 639.
54. Yuan, B.; Zhuang, J.; Kirmess, K. M.; Bridgmohan, C. N.; Whalley, A. C.; Wang, L.; Plunkett, K. N., Pentaleno[1,2-A:4,5′]Diacenaphthylenes: Uniquely Stabilized Pentalene Derivatives. *J. Org. Chem.* **2016**, *81*, 8312-8318.
55. Bheemireddy, S. R.; Ubaldo, P. C.; Finke, A. D.; Wang, L.; Plunkett, K. N., Contorted Aromatics Via a Palladium-Catalyzed Cyclopentannulation Strategy. *J. Mater. Chem. C* **2016**, *4*, 3963-3969.
56. Lu, L.; Zou, S.; Fang, B., The Critical Impacts of Ligands on Heterogeneous Nanocatalysis: A Review. *ACS Catal.* **2021**, *11*, 6020-6058.
57. Yang, T. H.; Shi, Y.; Janssen, A.; Xia, Y., Surface Capping Agents and Their Roles in Shape-Controlled Synthesis of Colloidal Metal Nanocrystals. *Angew. Chem. Int. Ed.* **2020**, *59*, 15378-15401.
58. Sirk, T. W.; Brown, E. F.; Sum, A. K.; Friedman, M., Molecular Dynamics Study on Biophysical Interaction of Seven Green Tea Catechins with Lipid Bilayers of Cell Membranes. *J. Agr. Food Chem.* **2008**, *56*, 7750-7758.
59. Evanoff Jr., D. D.; Chumanov, G., Synthesis and Optical Properties of Silver Nanoparticles and Arrays. *Chem. Phys. Chem.* **2005**, *6*, 1221-1331.
60. Xu, F.; Testoff, T. T.; Wang, L.; Zhou, X., Cause, Regulation and Utilization of Dye Aggregation in Dye-Sensitized Solar Cells. *Molecules* **2020**, *25*, 4478.
61. Xiao, L.; Wang, L., Structures of Platinum Clusters: Planar or Spherical? *J. Phys. Chem. A* **2004**, *108*, 8605-8614.
62. Xiao, L.; Tollberg, B.; Hu, X.; Wang, L., Structural Study of Gold Clusters. *J. Chem. Phys.* **2006**, *124*, 114309.
63. Xiao, L.; Wang, L., From Planar to Three-Dimensional Structural Transition in Gold Clusters and the Spin-Orbit Coupling Effect. *Chem. Phys. Lett.* **2004**, *392* 452-455.

64. Zhang, W.; Ge, Q.; Wang, L., Structure Effects on the Energetic, Electronic, and Magnetic Properties of Palladium Nanoparticles. *J. Chem. Phys.* **2003**, *118*, 5793-5801.
65. Shi, Y.; Lyu, Z.; Zhao, M.; Chen, R.; Nguyen, Q. N.; Xia, Y., Noble-Metal Nanocrystals with Controlled Shapes for Catalytic and Electrocatalytic Applications. *Chem. Rev.* **2021**, *121*, 649-735.
66. Miranda, R. R.; Sampaio, I.; Zucolotto, V., Exploring Silver Nanoparticles for Cancer Therapy and Diagnosis. *Colloids Surf. B: Biointerfaces* **2022**, *210*, 112254.
67. Yang, X.; Jia, M.; Li, Z.; Ma, Z.; Lv, J.; Jia, D.; He, D.; Zeng, R.; Luo, G.; Yu, Y., In-Situ Synthesis Silver Nanoparticles in Chitosan/Bletilla Striata Polysaccharide Composited Microneedles for Infected and Susceptible Wound Healing. *Int. J. Biolog. Macromol.* **2022**, *215*, 550-559.
68. Wang, L.; Kalyanaraman, C.; McCoy, A. B., Time-Dependent Quantum Studies of the $O(^3p)$+ Hcl Reaction. *J. Chem. Phys.* **1999**, *110*, 11221-11232.
69. Billing, G. D.; Wang, L., Semiclassical Calculations of Transport Coefficients and Rotational Relaxation of Nitrogen at High Temperatures. *J. Phys. Chem.* **1992**, *96*, 2572-2575.